Electronic Supplementary Material (ESI) for RSC Advances

SUPPORTING INFORMATION

Nonstoichiometric Bi_2O_3: Efficient Visible Light Photocatalyst

Shamaila Sajjad [a,b]*, Sajjad A. K. Leghari[a], Jinlong Zhang[a]

[a] Key Laboratory for Advanced Materials and Institute of Fine Chemicals, East China University of Science and Technology, 130 Meilong Road, Shanghai 200237, P.R. China.

[b] International Islamic University, H-10, Islamabad, Pakistan

E-mail: shalisajjad@hotmail.com

Experimental:

Experimental Approach: The pure Bi_2O_3 (Aldrich) (99.9%) with greenish yellow colour was treated in vacuum for 3h at 197.7 ^oC. The vacuum treatment of pure Bi_2O_3 for 3h at 197.7 ^oC is optimized according to different timings and temperature conditions. The vacuum oven (DZF-6020) is manufactured by Shanghai Hua-Lion equipment Co. Ltd. After this treatment, the color of the sample changed from greenish yellow to dark brown, which results in the formation of a new composite in the form of Bi_2O_3/ Bi_2O_{3+x}.

Catalyst Characterizations:

X-ray diffraction (XRD) analysis

The crystal phase composition and crystallinity of the obtained powder was determined by X-ray diffractometry (XRD) with Rigaku D/Max 2550 VB/PC apparatus (Cu Kα 1 radiation, λ = 0.154056nm) at room temperature operated at 40 kV and 100 mA. Diffraction patterns were recorded in the angular range of 20°-80º. The crystallite size was estimated by applying the Scherer equation to the full width at half-maximum (fwhm) of the (120) peak at 2θ= 27.4º of α-Bi_2O_3:

$$D = K\lambda/\beta\cos\theta$$

where β is the half-height width of the diffraction peak (FWHM), K = 0.89 is a coefficient, θ is the diffraction angle, and λ is the X-ray wavelength corresponding to the Cu K_α radiation. D is the average crystallite size of the powder sample in nanometer.

UV-vis diffuse reflectance spectra (DRS)

The UV-vis DRS spectra were obtained for the dry-pressed disk samples using a Scan UV-vis spectrophotometer (Varian, Cary 500, double beam spectrophotometer) equipped with an integrating sphere assembly, using $BaSO_4$ as the reflectance sample. The spectra were recorded at room temperature in air within the range 200-800 nm.

Raman spectra

Raman spectra of the samples were recorded by Renishaw inVia Raman spectrometer at room temperature with the excitation wavelength of 785 nm.

Thermogravimetric analysis (TGA)

Thermo gravimetric analysis (TGA) was performed on the Perkin-Elmer Pyris Diamond thermo gravimetric analyzer. TGA trace for the pure and vacuum treated samples was carried out at a heating rate of 10 ^oC/min from 40 to 800 ^oC in air.

Photoluminescence spectra (PLS)

Photoluminescence spectra were recorded by Varian Cary Eclipse Fluorescence spectrophotometer under the excitation light at 270 nm. The PL spectra of all samples were examined in the wavelength range of 300-800 nm.

X-ray photoelectron spectroscopy (XPS)

The instrument employed for XPS study was a Perkin-Elmer PHI 5000C ESCA System with Al K_α radiation operated at 250 W. Extended spectra were collected in the range 0-1000 eV. Detailed spectra were recorded for the following regions: C1s, Bi4f and O1s. The standard deviation in the BE values is ±0.05 eV. The raw spectra were fitted using a non-linear least-square fitting program adopting Gaussian-Lorentzian peak shapes for the peaks. In order to correct for charging effects, the BE values were referred to the C1s peak at 284.6 eV.

BET surface area analysis

Nitrogen adsorption and desorption isotherms were obtained at 77 K with a Micromeritics ASAP 2010 system. All the samples were degassed at 473 K before the measurement.

Electron paramagnetic resonance spectroscopy (EPR)

The electron paramagnetic resonance (EPR) spectra were recorded at 298 K using a Bruker EMX-8/2.7 EPR spectrometer operating at the X band and magnetic field modulation of 100 kHz, with a microwave power of 20.502 mW and modulation amplitude of 4.00 G. The microwave frequency of 9.86 GHz was read with a frequency counter.

Measurement of photocatalytic activity.

To evaluate the photocatalytic activities of these materials under visible light (λ>420 nm), oxidative decompositions of methylene blue (MB), methyl orange (MO) and nitro-phenol (NP) were tested. The 1000-Watt high-pressure W lamp was used as a visible light source mounted 10 cm away from the reaction solution. The short-wavelength components (λ < 420 nm) of the light were cut off using a cut-off glass filter. During the reaction, a water-cooling system cooled the water-jacketed photochemical reactor to maintain the solution at room temperature. The photocatalyst (0.05 g) was added into a 100 mL quartz photoreactor containing 50 mL of 10 mgL^{-1} aqueous solution of NP, MO and MB. The mixture was sonicated for 20 min and stirred for 30 min in the dark in order to reach the adsorption–desorption equilibrium. Preliminary studies indicated a linear light absorbance verse pollutant's concentration and that the decomposition of pollutant in the absence of photocatalyst or irradiation could be neglected. The reproducibility was checked by repeating the measurements at least three times and was found to be within the acceptable limit (±3 %). To analyze the concentration of organics, the suspension was first centrifuged and filtered through 0.22 μm Millipore membrane filters to remove the catalyst. The concentration of organics was measured with a UV–vis spectrophotometer (Varian Cary 100). The MB, MO and NP showed its main absorbance peak at 663, 465 and 273 nm, respectively.

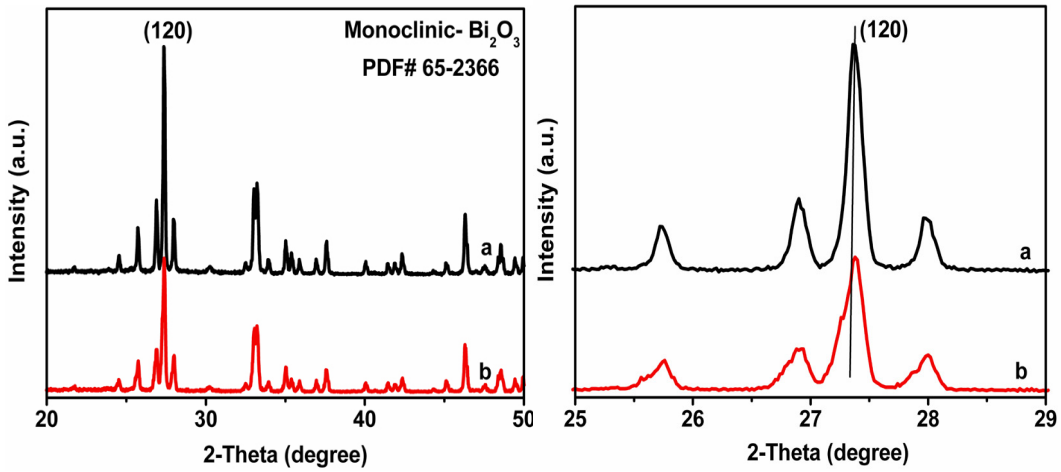

Figure S1. X-ray diffraction patterns of (a) pure Bi_2O_3; (b) Bi_2O_3/Bi_2O_{3+x} composite.

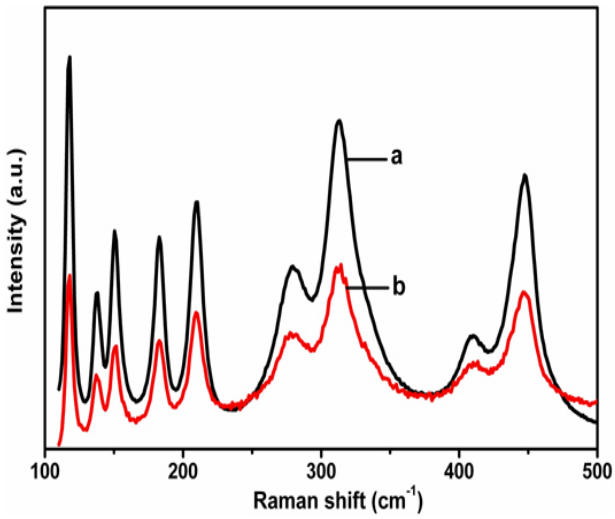

Figure S2. Raman spectra of (a) pure Bi_2O_3; (b) Bi_2O_3/Bi_2O_{3+x} composite.

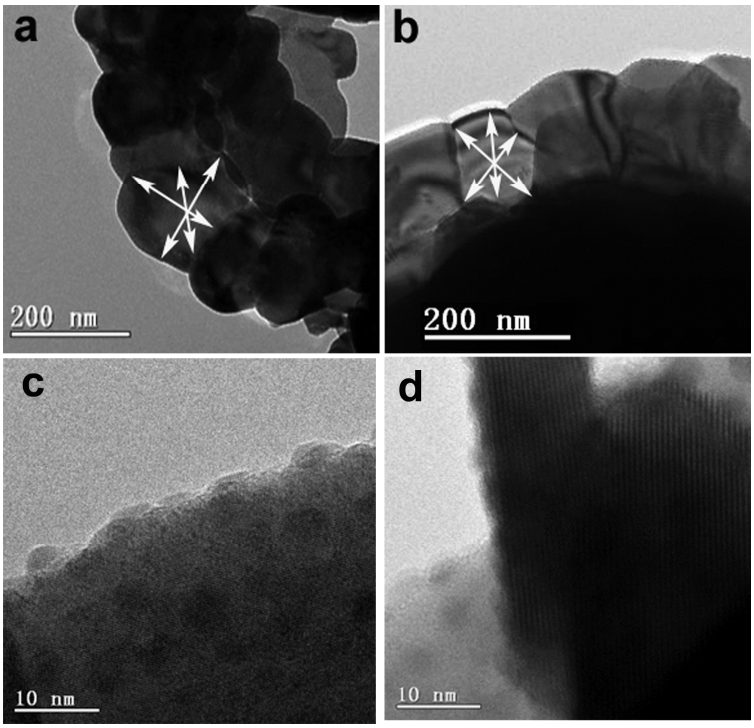

Figure S3. TEM and HRTEM images of (a) pure Bi_2O_3; (b) Bi_2O_3/Bi_2O_{3+x} composite; (c) pure Bi_2O_3; (d) Bi_2O_3/Bi_2O_{3+x} composite.

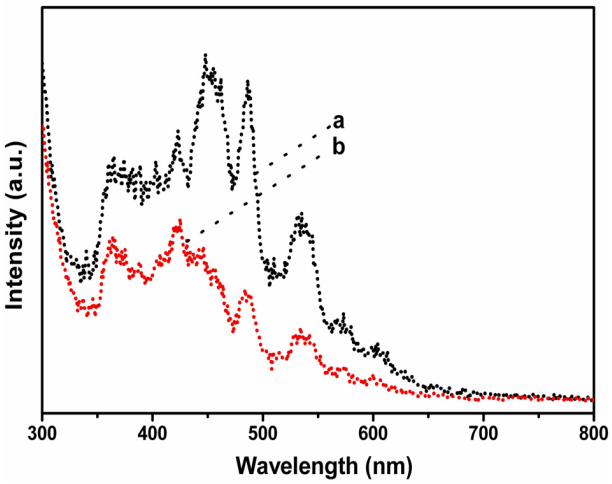

Figure S4. Photoluminescence spectra of (a) pure Bi_2O_3; (b) Bi_2O_3/Bi_2O_{3+x} composite.

.

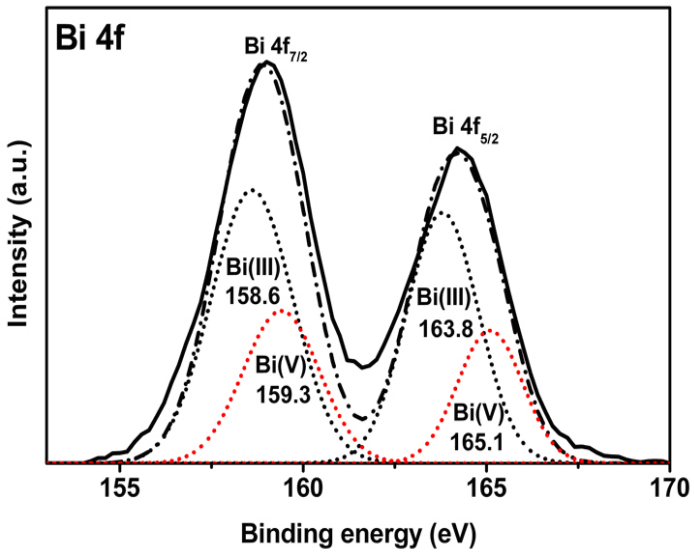

Figure S5. Deconvolution peaks of Bi 4f region of Bi_2O_3/Bi_2O_{3+x} composite

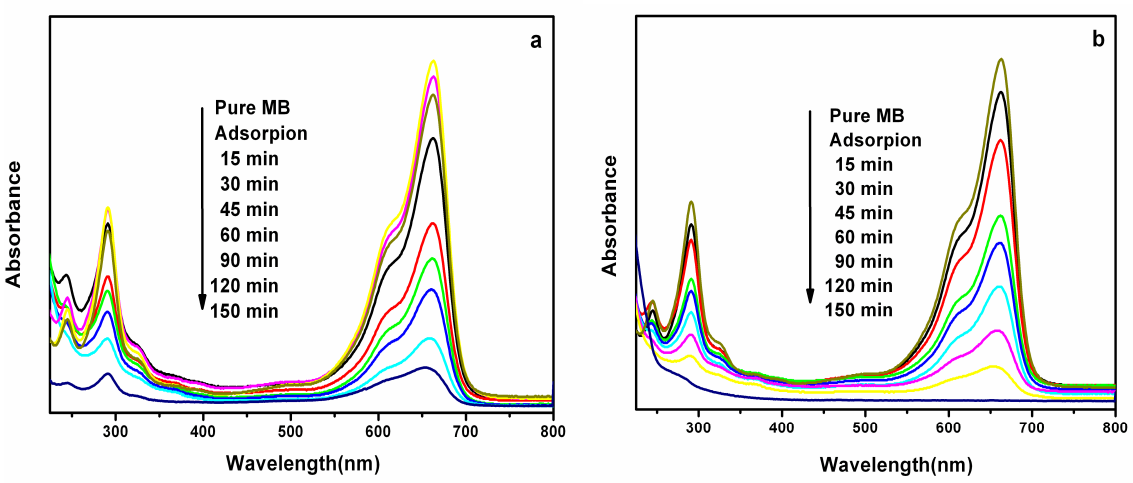

Figure S6. Degradation profile of methylene blue over (a) pure Bi_2O_3; (b) Bi_2O_3/Bi_2O_{3+x} composite.

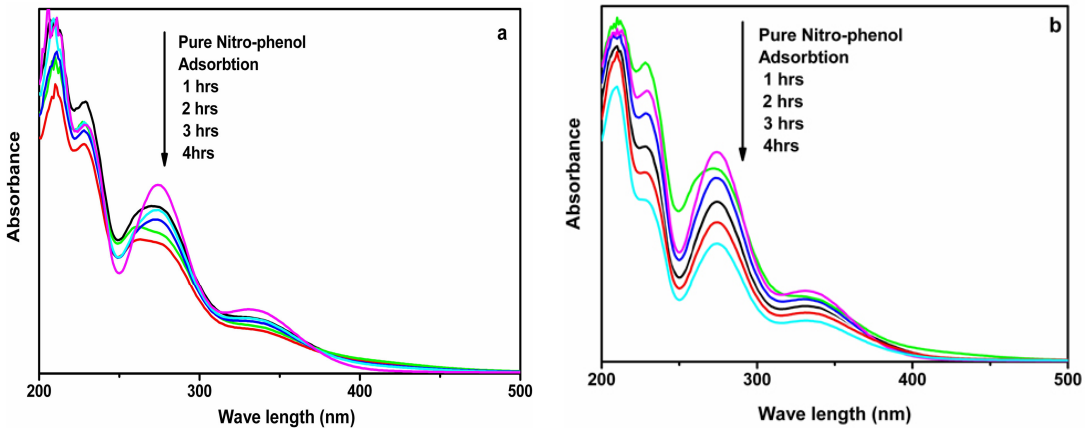

Figure S7. Degradation profile of nitro-phenol over (a) pure Bi_2O_3; (b) Bi_2O_3/Bi_2O_{3+x} composite.

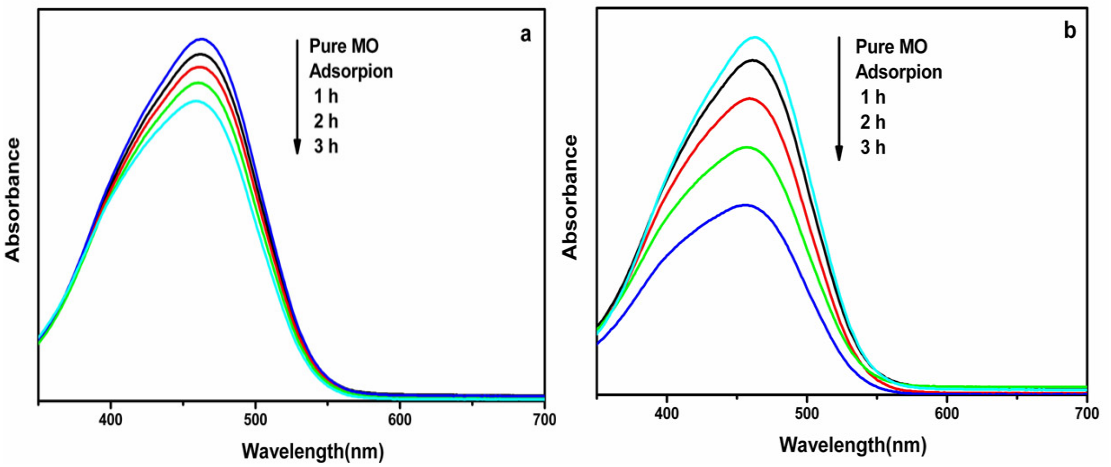

Figure S8. Degradation profile of methyl orange over (a) pure Bi_2O_3; (b) Bi_2O_3/Bi_2O_{3+x} composite.

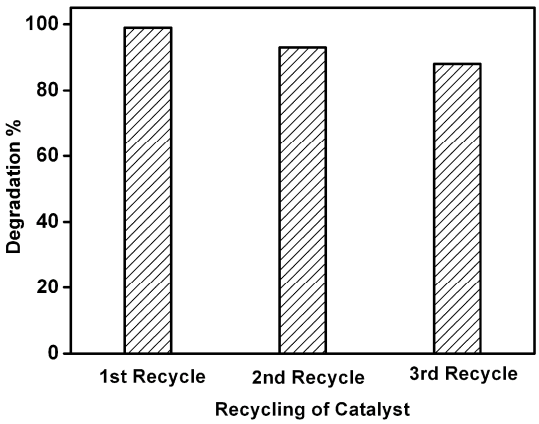

Figure S9. Recycling of Bi_2O_3/Bi_2O_{3+x} composite for the photo catalytic degradation of MO for 6 h visible light reaction illustrating photo stability.

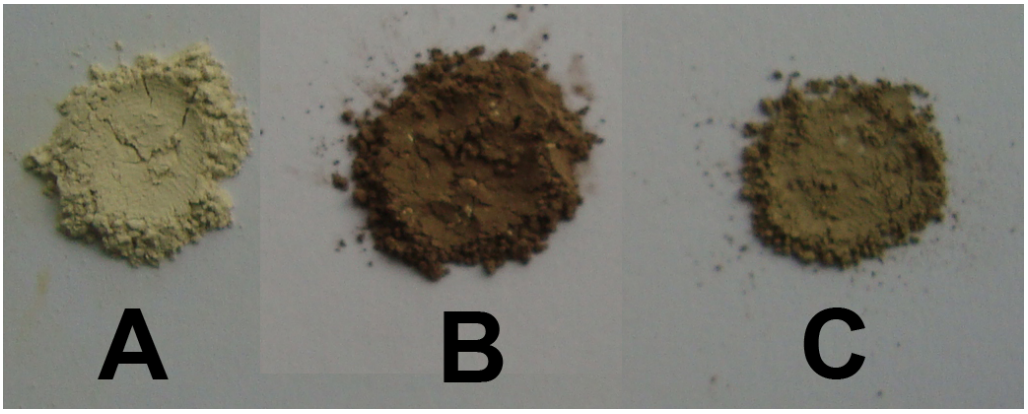

Figure S10. Photo graphs of pure Bi_2O_3, Bi_2O_3/Bi_2O_{3+x} composite and Bi_2O_3/Bi_2O_{3+x} composite after the photo catalytic degradation of MO for 6 h visible light reaction illustrating photo stability.

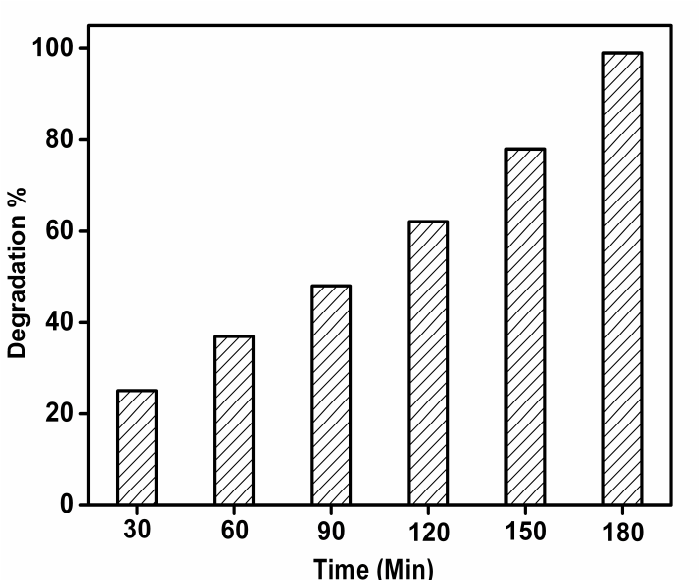

Figure S11. Photocatalytic degradation % of MO via Bi_2O_3/Bi_2O_{3+x} vacuum activated composite at different vacuum treatment timings.

Table S1: XRD parameters and crystallite sizes

Samples	2(θ)	FWHM	d(A)	Crystallite size (nm)	BET area (m^2g^{-1})
Pure Bi_2O_3	27.36	0.178	3.2501	105.40	0.57
Vac treated Bi_2O_3	27.42	0.234	3.2570	62.32	0.74